Self-Powered Triboelectric Nanosensor with Poly(tetrafluoroethylene) Nanoparticle Arrays for Dopamine Detection

Yang Jie,[†,‡,⊥] Ning Wang,[§,⊥] Xia Cao,[*,†,‡] Ying Xu,[‡,§] Tao Li,[‡] Xueji Zhang,[*,†] and Zhong Lin Wang[*,‡,∥]

[†]Research Center for Bioengineering and Sensing Technology, University of Science and Technology Beijing, Beijing 100083, China, [‡]Beijing Institute of Nanoenergy and Nanosystems, Chinese Academy of Sciences, Beijing 100083, China, [§]School of Chemistry and Environment, Beijing University of Aeronautics and Astronautics, Beijing 100191, China, and [∥]School of Material Science and Engineering, Georgia Institute of Technology, Atlanta, Georgia 30332-0245, United States. [⊥]Y.J. and N.W. contributed equally.

ABSTRACT A self-powered triboelectric nanosensor (TENS) based on the contact-separation mode between a thin layer of poly(tetrafluoroethylene) (PTFE) with nanoparticle arrays and an aluminum film was fabricated for the detection of dopamine (DA) in the alkaline condition. High selectivity and sensitivity (detection limit of 0.5 μM, a linear range from 10 μM to 1 mM) have been achieved through the strong interaction between the nonstick PTFE and DA *via* its oxidative self-polymerization, and the output voltage and current of the developed TENS can reach 116 V and 33 μA, which is exceptionally attractive for the fabrication of self-powered and portable device toward the detection of dopamine.

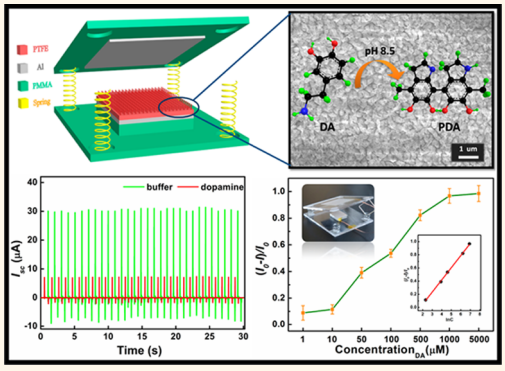

KEYWORDS: self-powered nanosensor · dopamine · poly(tetrafluoroethylene) nanoparticle arrays · triboelectric nanogenerator

Dopamine (3, 4-dihydroxyphenethylamine, DA) is one of the most significant catecholamines, which plays an important role in the central nervous, renal, and hormonal systems.[1,2] An abnormal level of dopamine may lead to neurological disorders, such as Parkinson's disease, Huntington's disease, and schizophrenia.[3−6] Multiple approaches, such as UV−vis spectrophotometry, high-performance liquid chromatography, fluorescence spectrophotometry, and electrochemical methods, have been applied to detect the dopamine in environmental and biological samples.[3,7−11] However, the sample preparation before measurement is rather complicated and time-consuming or requires expensive instrumentation. The coexistence of ascorbic acid (AA) and uric acid (UA) greatly renders electrochemical strategy very challenging.[9−11] It is still essential to develop simple and rapid methods for the determination of dopamine with high selectivity and simplicity in routine analysis.

In recent years, the concept of self-powered triboelectric nanosensor (TENS) has been proposed and tested for sensing mercury ions, catechin, and phenol.[12−14] The triboelectric effect is an old but well-known phenomenon that contact between two materials with different triboelectric polarities yields surface-charge transfer.[15] The working mechanism of TENS is based on combining and integrating a nanogenerator with a sensor.[16−18] The sensors can be driven by the energy harvested through the nanogenerators.[19] However, how to develop a fully integrated, stand-alone, and self-powered nanosensor is the major challenge.[15,20,21] As for the triboelectric nanogenerator (TENG), selecting the materials with the largest difference in the ability to attract electrons and changing the surface morphology are the key factors in maximizing

* Address correspondence to caoxia@ustb.edu.cn, zhangxueji@ustb.edu.cn, zlwang@gatech.edu.

Received for review May 20, 2015 and accepted July 26, 2015.

Published online 10.1021/acsnano.5b03052

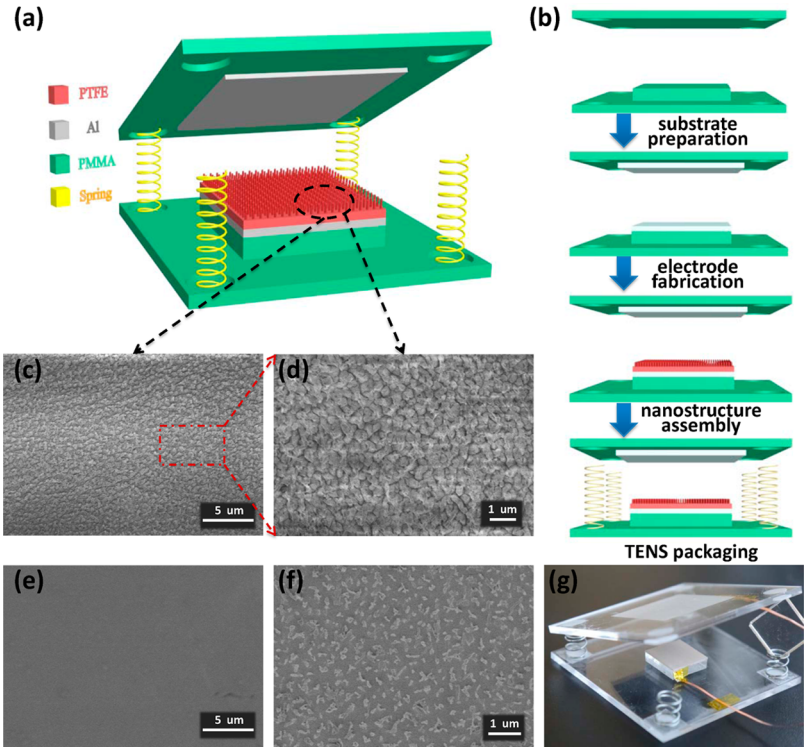

Figure 1. (a) Schematic illustration of the self-powered TENS. (b) Fabrication process of the self-powered TENS. (c–f) SEM images of the etched PTFE surface with nanoparticle array structure, except that (e) is the original PTFE surface. (g) Photograph of the fabricated self-powered TENS.

the charge generation.[15,22–26] Moreover, the strong interaction between polydopamine (PDA) and various membrane surfaces has attracted considerable interest.[27–30] A peculiar property of PDA is its ability to deposit onto virtually any type and shape of surface *via* the oxidative self-polymerization of dopamine at slightly basic pH. The PDA layer is hydrophilic, and its application decreases surface charge on some polymers.[31] Additionally, the qualitative presence of PDA films has been reported on a diversity of different materials, especially for poly(tetrafluoroethylene) (PTFE). PTFE is hydrophobic and nonstick because of its low surface energy. Furthermore, PTFE is the most electronegative material with a charge affinity of −190 nC/J, which was tested by Bill Lee (see Table 1, Supporting Information).

In this work, we demonstrate a new type of self-powered triboelectric nanosensors that can be used as a sensor for the detection of dopamine in the alkaline condition. By fully integrating the highly efficient TENG with the highly selective nonasensor, the output of TENS depends on the type and concentration of molecules adsorbed on the surface of the triboelectric material. The nanoparticle array structures of PTFE are designed as a triboelectric material in order to enhance the contact area and capture dopamine selectively in the alkaline solution, and the output voltage and current of this developed TENS can reach 116 V and 33 μA with an effective dimension of 2 cm × 2 cm. Under the optimum conditions, this TENS is selective for the determination of dopamine, with a detection limit of 0.5 μM and a linear range from 10 μM to 1 mM. Importantly, this study demonstrates an innovative and convenient method toward self-powered detection of dopamine.

RESULTS AND DISCUSSION

Here, we present a new type self-powered TENS that has a layered structure with two plates, as shown in Figure 1a. Poly(methyl methacrylate) (PMMA) was chosen as the substrate material because of its excellent impact strength, light weight, and easy handling. On the lower side, a sensitive element was prepared that has a much smaller dimension (2 cm × 2 cm) than the substrate. It consists of a thin layer of poly(tetrafluoroethylene) (PTFE) with nanoparticle array structure and a thin back electrode of aluminum (Al) film laminated between the substrate and PTFE. As sketched in Figure 1b, the fabrication flow is straightforward without sophisticated equipment and process. Specifically, the PTFE surface was etched to get the aligned nanoparticle arrays *via* the inductively coupled plasma (ICP) reactive ion-etching method. Usually, the output performance of the TENG can be enhanced by increasing the surface roughness and the effective surface area of the triboelectric materials to induce a larger triboelectric charge density.[12–14,24,26]

Figures 1c–f show a series of scanning electron microscopy (SEM) images of the PTFE thin film surface. Compared with the original PTFE surface (Figure 1e), a uniformly distributed nanoparticle arrays structure can be observed with an average diameter of about 300 nm (Figure 1c,d), but the nanoparticle arrays would be sparse due to the long-time etching, as shown in Figure 1f. In addition, Figure 1g shows the photograph of a real device. In this designed device, the PTFE and Al are extremely different in their ability to attract and retain electrons in the triboelectric series.[15,32]

The working mechanism of the TENS can be explained by the coupling between the triboelectric effect and electrostatic effect (Supporting Information, Figure S1). There exists an electric potential difference and an alternating current signal in external circuit with a periodical contact-separated process of the TENS. In theory, the TENS can be regarded as a flat-panel capacitor.[12,26,33] If the electric potential of the bottom side (U_{bottom}) is zero, the electric potential of the upper side (U_{upper}) can be expressed by

$$U_{upper} = -\frac{\sigma d}{\varepsilon_0} \quad (1)$$

where σ is the triboelectric charge density produced when the triboelectric materials contact, ε_0 is the vacuum permittivity, and d is the gap distance between the two panels. At open-circuit conditions, there is no charge transfer, and the open-circuit voltage (V_{oc}) equals the U_{upper}. Therefore, the V_{oc} will continue to increase until the maximum value is reached when the upper plate fully reverts to the original position. If the two electrodes are shorted, an instantaneous current is produced in order to balance the generated triboelectric potential. The induced charge density (σ') can be given by

$$\sigma' = \frac{\sigma d\varepsilon_1}{d_1 + d\varepsilon_1} = \frac{\sigma}{1 + \frac{d_1}{d\varepsilon_1}} \quad (2)$$

At short-circuit conditions, the short-circuit current (I_{sc}) can be calculated by

$$I_{sc} = \frac{S\sigma d_1 \varepsilon_1 v(t)}{(d_1 + d\varepsilon_1)^2} \quad (3)$$

where d_1 is the thickness of the PTFE film, ε_1 is the relative permittivity of PTFE, S is the effective contacting area of triboelectric material, and $v(t)$ is the average changing velocity of gap distance. In our experiments, the maximum gap distance of the TENS is set up to be 15 mm.

The output of TENS is closely related to the surface profile and the ability to gain/lose electrons of the triboelectric material.[15] Materials with large (hyper)polarizabilities generally exhibit significantly higher dielectric responses in previous work.[34] The surface of PTFE can be modified *via* the oxidative self-polymerization of dopamine at slightly basic pH, although it is hydrophobic and nonstick due to the low surface energy. In addition, the nitrogen and oxygen functional groups containing polymers develop the positive charge, and the halogenated polymers develop the negative charge.[32] Therefore, the designed TENS can be effective and sensitive to detection of dopamine as the adsorbed PDA on PTFE would change the permittivity and the surface electrification.

As sketched in Figure 2a, the dopamine polymerization mechanism mainly involves the oxidation of catechol in dopamine to dopamine–quinone by alkaline pH-induced oxidation and the cross-linking of dopamine–quinone.[27] First, the dopamine was oxidized to dopamine–quinone; next, the intramolecular cyclization of the dopamine–quinone led to the leukodopaminechrome *via* 1,4-Michael addition; and then leukodopaminechrome was further oxidized and rearranged to 5,6-dihydroxyindole, whose further oxidation caused intermolcular cross-linking to yield polydopamine. The primary roles of adhesive bonding and cross-link formation can be assigned to the reverse dismutation reaction between catechol and *o*-quinone form of DA.

When the surface of the working electrode is modified by PDA, the thickness and permittivity of this modification would change the output of TENS. There exists a variation of the triboelectric charge density because σ is mainly affected by the intrinsic properties of the two triboelectric layers and roughness of the contact surfaces. The I_{sc} can be calculated by

$$I_{sc} = \frac{S\sigma d_{11} \varepsilon_{11} v(t)}{(d_{11} + d\varepsilon_{11})^2} \quad (4)$$

where d_{11} and ε_{11} are the thickness of the PTFE and the relative permittivity of PTFE after modification with PDA, respectively.

In the experiment, the fabricated PTFE with nanoparticle array structure was soaked with the tris(hydroxymethyl)aminomethane (TRIS) buffer solution (pH = 8.5) containing various concentrations of dopamine and other interference factors at ambient temperature (Figure 2b). After being soaked for a certain time, the PTFE plate was washed with water and dried at ambient temperature prior to electrical measurement. The insets (i) and (ii) in Figure 2b show the changes of color and hydrophobicity of PTFE after being soaked in the dopamine solution, respectively. The absorption intensity for the polymerization increases with time, and thus, the color of the DA solution and surface of PTFE has a gradual change from colorless to dark brown. Moreover, the surface properties of PTFE and the output of TENS changed with the deposition of PDA, and thus, the TENS can be a sensor for the detection of dopamine in the alkaline condition.

The TENS was mechanically tested by a homemade motor system that applied periodical compressive

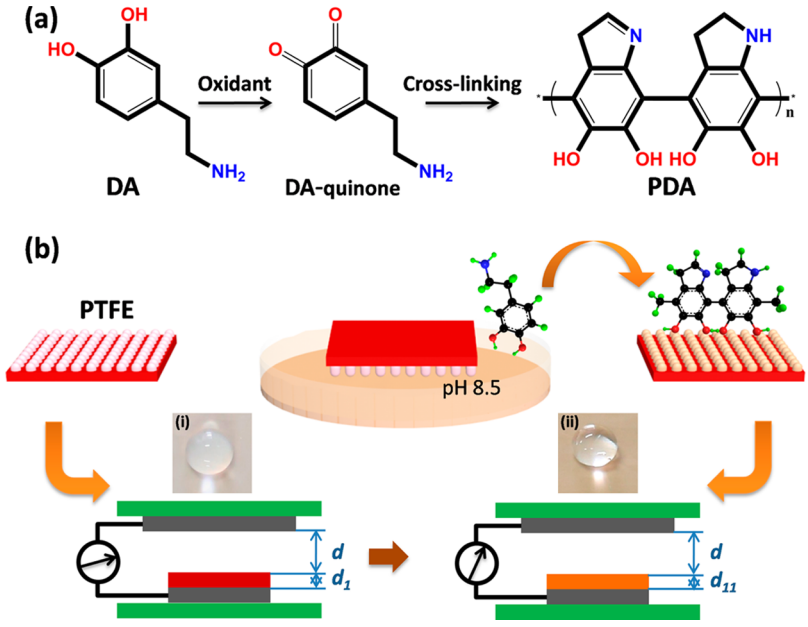

Figure 2. (a) Schematic illustration of the reaction mechanism of DA *via* the oxidative self-polymerization. (b) Schematic illustration of the deposition of PDA and the work of TENS by dip-coating the PTFE with nanoparticle arrays structure in an alkaline dopamine solution (pH 8.5). Inset: Photographs of water droplet on the surface of PTFE (i) before and (ii) after the soaking.

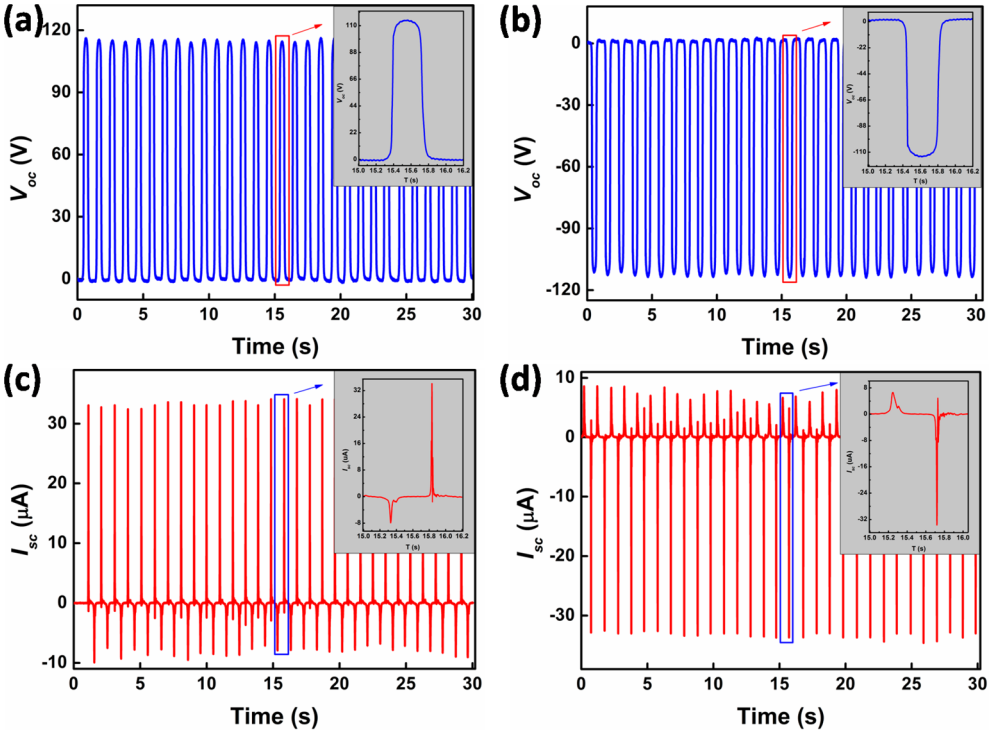

Figure 3. (a, b) Generated open-circuit voltage and (c, d) short-circuit current of the TENS at opposite connection to the measurement system. Insets (a–d): enlarged view of one cycle.

force. Experimentally, both the open-circuit voltage (V_{oc}) and the short-circuit current (I_{sc}) of the TENS (PTFE condition: 40 s ICP etching time; 2 cm × 2 cm area) are maximized with controlled force (60 N) at a vibration frequency of 1 Hz with maximum values of 116 V and 33 μA, respectively. From the enlarged view of Figure 3a, a positive voltage of 116 V is generated because of the immediate charge separation, and it holds at a plateau until the subsequent pressing deformation. As manifested in the inset of Figure 3c, the peak value of I_{sc} reaches 33 μA, corresponding to the half cycle of pressing that is at a higher straining rate than releasing. By measuring with a reverse connection to the electrometer, it can be proved that the

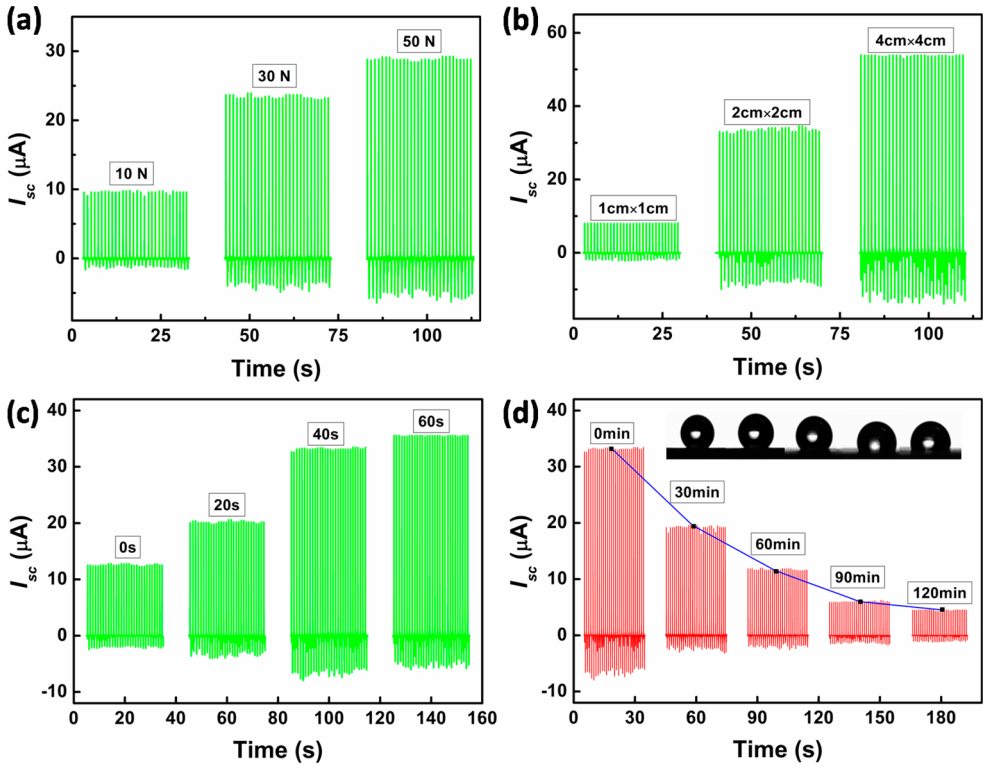

Figure 4. (a) Generated short-circuit current of the TENS (2 cm × 2 cm PTFE etched by ICP for 40 s) under different applied force. (b) Generated short-circuit current of the TENS (ICP for 40 s) fabricated with different area of PTFE. (c) Generated short-circuit current of the TENS (2 cm × 2 cm) fabricated with PTFE etched by ICP for different lengths of time. (d) Generated short-circuit current of the developed TENS reacting with 500 μM dopamine for different lengths of time. Inset: Change of water droplet profile after the surfaces of PTFE reacted with dopamine.

signals were generated by the TENS (Figure 3b,d). Thus, the TENS has a distinct competitive advantage in the further fabrication of self-powered and portable devices toward the detection of dopamine.

In order to get the stable and optimized TENS, some important factors were investigated including the applied force, the contact area, and the ICP time. As shown in Figure 4a, the larger applied force would produce higher electrical output until a saturated limit is reached because the output of the TENS greatly depends on the force. In the subsequent testing experiments, a controlled force of 60 N was applied. In addition, Figure 4b shows that the short-circuit current of TENS increased upon increasing the area of PTFE (40 s ICP etching time). When the TENS is used for the determination of dopamine, the area of PTFE would be better to be smaller in order to check a tiny volume, and 2 cm × 2 cm was designed as the effective dimension. Moreover, the electric signals of TENS with PTFE (2 cm × 2 cm) etched by ICP in different time were compared as shown in Figure 4c. After etching by ICP, the short circuit current of TENS is enhanced, and it verifies that the electrical output is related to the contact area. The nanostructure of the PTFE surface can greatly change the effective contact area and the triboelectric charge density as well as the total electric output of the device. However, when the etching time was more than 40 s, the I_{sc} would increase slightly. The reason could be that the densities of different-sized nanoparticles generated by different ICP etching time are similar (Supporting Information, Figure S2). Considering the cost efficiency and electrical output of each TENS, 40 s is chosen as the etching time.

Next, the optimum TENS was used to detect the dopamine. Figure 4d shows that the generated short-circuit current of the developed TENS is greatly related to the reacting time with dopamine. It had been demonstrated that the oxidative self-polymerization of dopamine is a function of the immersion time, and the PDA coating was independent of the substrate composition.[27−29,35] However, the I_{sc} decreased slowly when the reacting time continued for more than 90 min. Thus, the reaction time was optimized to 90 min. Moreover, the surface hydrophilicity of PTFE was investigated by water contact angle measurement. The inset in Figure 4d shows the change of water droplet profile after the surfaces of PTFE reacted with dopamine, but the change of contact angle value was much less significant than the output of TENS (see Table 2, Supporting Information). It also demonstrates that the surface of PTFE was changed after reaction with different concentrations of dopamine.

The generated short-circuit current of the TENS declines when the dopamine (500 μM) solution was

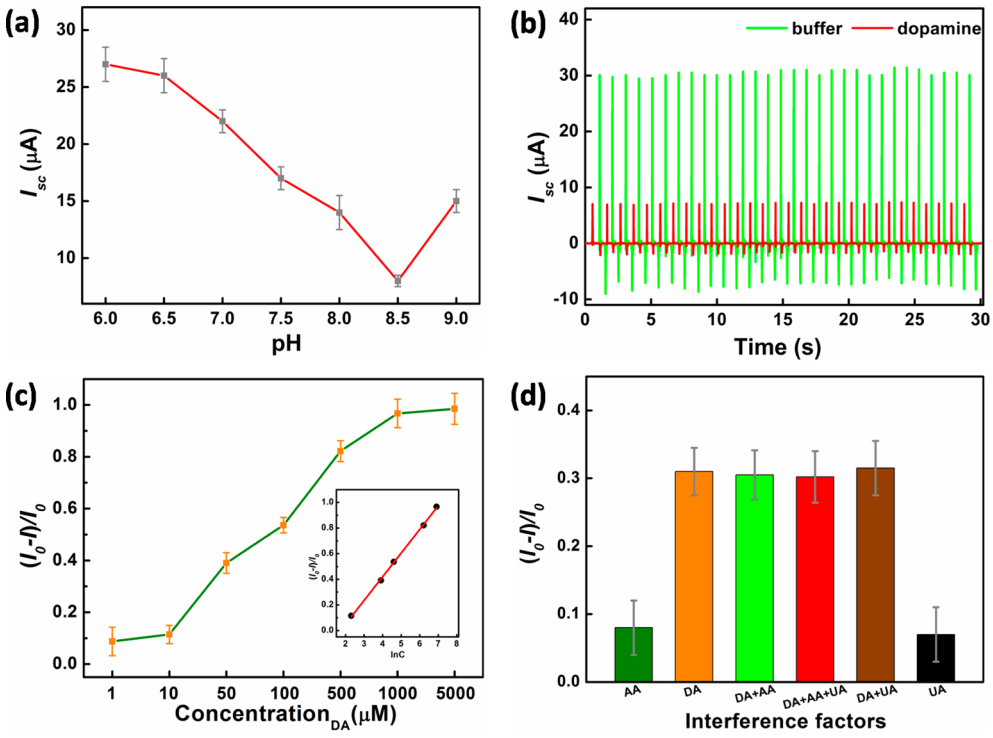

Figure 5. (a) Effect of dopamine (500 μM) solution pH on the generated short-circuit current of the developed TENS. (b) Results of comparing experiment between the TRIS buffer (pH = 8.5) and dopamine (500 μM) solution. (c) Sensitivity of the optimum TENS in the detection of dopamine. Inset: a linear relationship between the short circuit current ratio ($(I_0 - I)/I_0$) and the Napierian logarithm of the concentration of dopamine. (d) Selectivity of the optimum TENS for dopamine with the interference factors including ascorbic acid and uric acid. The concentration of all factors tested in the selectivity experiment was 30 μM.

changed from acid to alkaline as shown in Figure 5a. It can be explained that the alkaline condition stimulated the oxidation of catechol to the quinine form (Figure 2a). This verified the dominant role of PDA to alter triboelectric signals in the dopamine detection processing, and the minimum I_{sc} was generated at pH 8.5, which confirms the aforementioned mechanism about the dopamine polymerization.[27,29,35] In addition, the electrical signal of the TENS would decrease slightly after contact with solution, resulting in a negligible change even when the plate was dried intensively. It could be explained that the original accumulated triboelectric charging of PTFE was removed by solution. The original accumulated triboelectric charging of PTFE could be achieved by the process of ICP due to the prior-charge injection and triboelectrification with plasma.[36,37] Comparison experiments were carried out to study the change of I_{sc} between the TRIS buffer (pH = 8.5) and dopamine (500 μM) solution, and the results are shown in Figure 5b. After reaction with the dopamine, the generated I_{sc} of TENS decreased from 30 μA to 8 μA, which reflected the strong interaction between the dopamine and PTFE.

It is worth noting that triboelectric charges of TENS are very dependent on the surface properties of the contacting surfaces. Figure 5c manifests the electrical signal of the TENS increased upon decreasing the concentration of dopamine, with a linear relationship (inset) between the short circuit current ratio ($(I_0 - I)/I_0$) and the Napierian logarithm of the concentration of dopamine ranging from 10 μM to 1 mM ($R^2 = 0.99$). This type of TENS has a detection limit of 0.5 μM for dopamine, which indicates that the PDA-diminished triboelectrification is an effective means for DA detection. Although further low concentration detection of dopamine can be achieved by microminiaturization of TENS, the designed TENS has the portable and convenient advantages in the general test approach. In addition, the speed of dopamine polymerization in extremely low concentration is also the sensing limitation.

Control experiments were carried out to test the selectivity of the developed TENS toward dopamine detection as compared to other interference factors. As the solubility of uric acid is 0.0006 g/100 mL (at 20 °C), each interference factor was detected at a concentration of 30 μM. The results reveal that the developed TENS is specific to dopamine as shown in Figure 5d. Compared to the ascorbic acid and uric acid, only the dopamine can react with the PTFE and change the output of the TENS. In current electrochemical detections of DA, the sensitivity and selectivity suffer from a fouling effect due to the oxidation properties of AA and UA. However, the AA and UA, like many other molecules, have extremely poor interactions with the PTFE, and thus, the TENS has intelligent signal-to-noise ratio.

CONCLUSIONS

In summary, we have demonstrated a triboelectric effect based nanosensor for the selective detection of dopamine by utilizing PTFE with nanoparticle arrays structure as the sensitive element and contact material. This novel TENS is highly sensitive (detection limit of 0.5 μM and linear range of 10 μM to 1 mM) and selective for dopamine, which holds great potential for the determination of dopamine in conventional samples. Among the currently proposed detecting methods of dopamine, this study is the first to integrate the TENG performance and nanosensor in the alkaline conditions. Considering its high selectivity, sensitivity, and simplicity, we believe the innovative mechanism of TENS will serve as the stepping stone for related TENS studies and contribute to the future development of self-powered nanosensors.

METHODS

Reagents and Chemicals. All reagents and chemicals were analytical grade, purchased from Sigma-Aldrich, and were directly used for the following experiments. Deionized water with a resistivity greater than 18.0 MΩ was used in all of the assays and solutions. DA hydrochloride, AA, and UA solutions were prepared daily and stored in a refrigerator. In the investigation of the effect of pH on the generated short-circuit current of the developed TENS, the dopamine solution with pH range 6.0−7.0 was prepared by a phosphate (Na_2HPO_4 + KH_2PO_4) buffer solution, while the solution with a pH value of 7.5−9.0 was prepared by a Tris-HCl buffer solution.

Nanoparticle Arrays of PTFE Surface Modification. The nanoparticle array structure with an average diameter of about 300 nm on the PTFE (0.15 mm) surface was fabricated by using the inductively coupled plasma (ICP) reactive ion etching. Before the etching process, a thin Au film with a thickness of about 50 nm as the mask was deposited on the PTFE surface. A mixed gas including Ar, O_2, and CF_4 was introduced in the ICP chamber, where the corresponding flow rates are 15.0, 10.0, and 30.0 sccm, respectively. The PTFE nanoparticle arrays structure was etched under one power source of 400 W to generate a large density of plasma.

Fabrication of TENS. A thin film of Al (about 50 nm) was deposited on the other side of the PTFE layer with nanoparticle arrays by an e-beam evaporator, and the Al/PTFE composite film was cut into square pieces with dimensions of 1 cm × 1 cm, 2 cm × 2 cm, and 4 cm × 4 cm. The Al/PTFE composite piece was then glued to the inner surface of the PMMA substrate. This is the lower side (sensitive element of the TENS). On the other plate, another larger Al thin film was deposited through an open window area of the rectangular mask, and it played dual roles for contact material and electrode. The two plates were connected by four springs installed at the corners, leaving a narrow spacing between the contact electrode and the PTFE. The gap distance was designed to be 15 mm. Finally, conducting wires were connected to the two electrodes as leads for subsequent electrical measurements.

Characterization. The surface morphology of the PTFE thin film was characterized by a SU8020 field emission scanning electron microscope. For the measurement of the electric outputs of the TENS, an external force was applied by a commercial linear mechanical motor, and there would be friction between the PTFE thin film and paper, resulting in triboelectric potential and electric output in the external circuit. The open-circuit voltage was measured by using a Keithley Model 6514 system electrometer, while the short circuit current was measured by using an SR570 low-noise current amplifier (Stanford Research System). The water contact angle measurement was accomplished by use of an OCA40 Micro Data Physics Instrument (GmbH Germany) and OCA20 Contact Angle System (25 °C and 60% relative humidity).

Conflict of Interest: The authors declare no competing financial interest.

Acknowledgment. We acknowledge financial support from the National Natural Science Foundation of China (NSFC Nos. 21275102, 21173017, and 51272011), the Program for New Century Excellent Talents in University (NCET-12-0610), the Science and Technology Research Projects from Education Ministry (213002A), National "Twelfth Five-Year" Plan for Science & Technology Support (No. 2013BAK12B06), the "Thousands Talents" Program for Pioneer Researcher and His Innovation Team, China, and the National Natural Science Foundation of China (Grant Nos. 51432005 and Y4YR011001).

Supporting Information Available: The Supporting Information is available free of charge on the ACS Publications website at DOI: 10.1021/acsnano.5b03052.

Additional information, figures, and tables (PDF)

REFERENCES AND NOTES

1. Phillips, P. E. M.; Stuber, G. D.; Heien, M. L. A. V.; Wightman, R. M.; Carelli, R. M. Subsecond Dopamine Release Promotes Cocaine Seeking. *Nature* **2003**, *422*, 614–618.
2. Howe, M. W.; Tierney, P. L.; Sandberg, S. G.; Phillips, P. E. M.; Graybiel, A. M. Prolonged Dopamine Signalling in Striatum Signals Proximity and Value of Distant Rewards. *Nature* **2013**, *500*, 575–579.
3. Lee, T.; Cai, L. X.; Lelyveld, V. S.; Hai, A.; Jasanoff, A. Molecular-Level Functional Magnetic Resonance Imaging of Dopaminergic Signaling. *Science* **2014**, *344*, 533–535.
4. Santana, M. B.; Halje, P.; Simplicio, H.; Richter, U.; Freire, M. A. M.; Petersson, P.; Fuentes, R.; Nicolelis, M. A. L. Spinal Cord Stimulation Alleviates Motor Deficits in a Primate Model of Parkinson Disease. *Neuron* **2014**, *84*, 716–722.
5. Schubert, C. R.; Xi, H. S.; Wendland, J. R.; O'Donnell, P. Translating Human Genetics into Novel Treatment Targets for Schizophrenia. *Neuron* **2014**, *84*, 537–541.
6. Lammel, S.; Steinberg, E. E.; Földy, C.; Wall, N. R.; Beier, K.; Luo, L.; Malenka, R. C. Diversity of Transgenic Mouse Models for Selective Targeting of Midbrain Dopamine Neurons. *Neuron* **2015**, *85*, 429–438.
7. VanDersarl, J. J.; Mercanzini, A.; Renaud, P. Integration of 2d and 3d Thin Film Glassy Carbon Electrode Arrays for Electrochemical Dopamine Sensing in Flexible Neuroelectronic Implants. *Adv. Funct. Mater.* **2015**, *25*, 78–84.
8. Zhang, M.; Liao, C.; Yao, Y.; Liu, Z.; Gong, F.; Yan, F. High-Performance Dopamine Sensors Based on Wholegraphene Solution- Gated Transistors. *Adv. Funct. Mater.* **2014**, *24*, 978–985.
9. Li, B.-R.; Hsieh, Y.-J.; Chen, Y.-X.; Chung, Y.-T.; Pan, C.-Y.; Chen, Y.-T. An Ultrasensitive Nanowire-Transistor Biosensor for Detecting Dopamine Release from Living Pc12 Cells under Hypoxic Stimulation. *J. Am. Chem. Soc.* **2013**, *135*, 16034–16037.
10. Yue, H. Y.; Huang, S.; Chang, J.; Heo, C.; Yao, F.; Adhikari, S.; Gunes, F.; Liu, L. C.; Lee, T. H.; Oh, E. S.; et al. Zno Nanowire Arrays on 3d Hierachical Graphene Foam: Biomarker Detection of Parkinson's Disease. *ACS Nano* **2014**, *8*, 1639–1646.
11. Weng, J.; Xue, J. M.; Wang, J.; Ye, J. S.; Cui, H. F.; Sheu, F. S.; Zhang, Q. Q. Gold-Cluster Sensors Formed Electrochemically at Boron-Doped-Diamond Electrodes: Detection of Dopamine in the Presence of Ascorbic Acid and Thiols. *Adv. Funct. Mater.* **2005**, *15*, 639–647.

12. Lin, Z. H.; Xie, Y.; Yang, Y.; Wang, S.; Zhu, G.; Wang, Z. L. Enhanced Triboelectric Nanogenerators and Triboelectric Nanosensor Using Chemically Modified Tio2 Nanomaterials. *ACS Nano* **2013**, *7*, 4554–4560.
13. Lin, Z.-H.; Zhu, G.; Zhou, Y. S.; Yang, Y.; Bai, P.; Chen, J.; Wang, Z. L. A Self-Powered Triboelectric Nanosensor for Mercury Ion Detection. *Angew. Chem.* **2013**, *125*, 5169–5173.
14. Li, Z.; Chen, J.; Yang, J.; Su, Y.; Fan, X.; Wu, Y.; Yu, C.; Wang, Z. L. B-Cyclodextrin Enhanced Triboelectrification for Self-Powered Phenol Detection and Electrochemical Degradation. *Energy Environ. Sci.* **2015**, *8*, 887–896.
15. Wang, Z. L. Triboelectric Nanogenerators as New Energy Technology for Self-Powered Systems and as Active Mechanical and Chemical Sensors. *ACS Nano* **2013**, *7*, 9533–9557.
16. Zhang, H.; Yang, Y.; Hou, T.-C.; Su, Y.; Hu, C.; Wang, Z. L. Triboelectric Nanogenerator Built inside Clothes for Self-Powered Glucose Biosensors. *Nano Energy* **2013**, *2*, 1019–1024.
17. Zhang, H.; Yang, Y.; Su, Y.; Chen, J.; Hu, C.; Wu, Z.; Liu, Y.; Wong, C. P.; Bando, Y.; Wang, Z. L. Triboelectric Nanogenerator as Self-Powered Active Sensors for Detecting Liquid/Gaseous Water/Ethanol. *Nano Energy* **2013**, *2*, 693–701.
18. Meng, B.; Tang, W.; Too, Z.-h.; Zhang, X.; Han, M.; Liu, W.; Zhang, H. A Transparent Single-Friction-Surface Triboelectric Generator and Self-Powered Touch Sensor. *Energy Environ. Sci.* **2013**, *6*, 3235–3240.
19. Lee, M.; Bae, J.; Lee, J.; Lee, C.-S.; Hong, S.; Wang, Z. L. Self-Powered Environmental Sensor System Driven by Nanogenerators. *Energy Environ. Sci.* **2011**, *4*, 3359–3363.
20. Zi, Y.; Lin, L.; Wang, J.; Wang, S.; Chen, J.; Fan, X.; Yang, P.-K.; Yi, F.; Wang, Z. L. Triboelectric-Pyroelectric-Piezoelectric Hybrid Cell for High-Efficiency Energy-Harvesting and Self-Powered Sensing. *Adv. Mater.* **2015**, *27*, 2340–2347.
21. Su, Y.; Zhu, G.; Yang, W.; Yang, J.; Chen, J.; Jing, Q.; Wu, Z.; Jiang, Y.; Wang, Z. L. Triboelectric Sensor for Self-Powered Tracking of Object Motion inside Tubing. *ACS Nano* **2014**, *8*, 3843–3850.
22. Yang, Y.; Zhang, H.; Chen, J.; Jing, Q.; Zhou, Y. S.; Wen, X.; Wang, Z. L. Single-Electrode-Based Sliding Triboelectric Nanogenerator for Self-Powered Displacement Vector Sensor System. *ACS Nano* **2013**, *7*, 7342–7351.
23. Yang, P. K.; Lin, Z. H.; Pradel, K. C.; Lin, L.; Li, X.; Wen, X.; He, J. H.; Wang, Z. L. Paper-Based Origami Triboelectric Nanogenerators and Self-Powered Pressure Sensors. *ACS Nano* **2015**, *9*, 901–907.
24. Chen, J.; Zhu, G.; Yang, W.; Jing, Q.; Bai, P.; Yang, Y.; Hou, T.-C.; Wang, Z. L. Harmonic-Resonator-Based Triboelectric Nanogenerator as a Sustainable Power Source and a Self-Powered Active Vibration Sensor. *Adv. Mater.* **2013**, *25*, 6094–6099.
25. Yang, W.; Chen, J.; Zhu, G.; Yang, J.; Bai, P.; Su, Y.; Jing, Q.; Cao, X.; Wang, Z. L. Harvesting Energy from the Natural Vibration of Human Walking. *ACS Nano* **2013**, *7*, 11317–11324.
26. Zhu, G.; Lin, Z.-H.; Jing, Q.; Bai, P.; Pan, C.; Yang, Y.; Zhou, Y.; Wang, Z. L. Toward Large-Scale Energy Harvesting by a Nanoparticle-Enhanced Triboelectric Nanogenerator. *Nano Lett.* **2013**, *13*, 847–853.
27. Lee, H.; Dellatore, S. M.; Miller, W. M.; Messersmith, P. B. Mussel-Inspired Surface Chemistry for Multifunctional Coatings. *Science* **2007**, *318*, 426–430.
28. Hong, S.; Na, Y. S.; Choi, S.; Song, I. T.; Kim, W. Y.; Lee, H. Non-Covalent Self-Assembly and Covalent Polymerization Co-Contribute to Polydopamine Formation. *Adv. Funct. Mater.* **2012**, *22*, 4711–4717.
29. Lee, H.; Lee, B. P.; Messersmith, P. B. A Reversible Wet/Dry Adhesive Inspired by Mussels and Geckos. *Nature* **2007**, *448*, 338–341.
30. Lee, H.; Scherer, N. F.; Messersmith, P. B. Single-Molecule Mechanics of Mussel Adhesion. *Proc. Natl. Acad. Sci. U. S. A.* **2006**, *103*, 12999–13003.
31. Xiao, Y.; Zai, J.; Li, X.; Gong, Y.; Li, B.; Han, Q.; Qian, X. Polydopamine Functionalized Graphene/Nife2o4 Nanocomposite with Improving Li Storage Performances. *Nano Energy* **2014**, *6*, 51–58.
32. Diaz, A. F.; Felix-Navarro, R. M. A Semi-Quantitative Tribo-Electric Series for Polymeric Materials: The Influence of Chemical Structure and Properties. *J. Electrost.* **2004**, *62*, 277–290.
33. Zhong, J.; Zhong, Q.; Fan, F.; Zhang, Y.; Wang, S.; Hu, B.; Wang, Z. L.; Zhou, J. Finger Typing Driven Triboelectric Nanogenerator and Its Use for Instantaneously Lighting up Leds. *Nano Energy* **2013**, *2*, 491–497.
34. Heitzer, H. M.; Marks, T. J.; Ratner, M. A. Molecular Donor-Bridge-Acceptor Strategies for High-Capacitance Organic Dielectric Materials. *J. Am. Chem. Soc.* **2015**, *137*, 7189–7196.
35. Ryu, J.; Ku, S. H.; Lee, H.; Park, C. B. Mussel-Inspired Polydopamine Coating as a Universal Route to Hydroxyapatite Crystallization. *Adv. Funct. Mater.* **2010**, *20*, 2132–2139.
36. Wang, Z.; Cheng, L.; Zheng, Y.; Qin, Y.; Wang, Z. L. Enhancing the Performance of Triboelectric Nanogenerator through Prior-Charge Injection and Its Application on Self-Powered Anticorrosion. *Nano Energy* **2014**, *10*, 37–43.
37. Zhang, X.-S.; Han, M.-D.; Wang, R.-X.; Meng, B.; Zhu, F.-Y.; Sun, X.-M.; Hu, W.; Wang, W.; Li, Z.-H.; Zhang, H.-X. High-Performance Triboelectric Nanogenerator with Enhanced Energy Density Based on Single-Step Fluorocarbon Plasma Treatment. *Nano Energy* **2014**, *4*, 123–131.